

Correlation of Projected Flame Height for Impinging Horizontal Jet Flames

Nur Shahidah Ab Aziz^{a,*}, Rafiziana Md. Kasmani^b, Nor Roslina Rosli^a

^aSchool of Chemical Engineering, College of Engineering, Universiti Teknologi MARA, Malaysia

^bDepartment of Energy Engineering, Faculty of Chemical and Energy Engineering, Universiti Teknologi Malaysia, Malaysia
 shahidah_aziz@uitm.edu.my

Horizontal jet flame is said to be among the most dangerous types of fire considering a possible impingement effect on nearby facilities. Numerous studies have been conducted and assessed for geometrical flame features of jet flames as it imposed dangers where nearby equipment is included. However, data on flame height are often missing considering the effects may be deteriorative in the presence of nearby equipment. This study was carried out by using propane as fuel and the jet fire was released from a circular nozzle (diameter of 7.15 mm and 9.8 mm). The purpose is to determine a suitable correlation to be used to predict the flame extension length in the case of an impingement scenario. A review of the literature revealed that existing correlations are inapplicable to impinging jet fires. This study offers a better correlation which used elliptical flame shape assumption as a basis. A new correlation was suggested based on the experimental condition which is

$$\frac{H_p}{d} \sim 31.4 \left[\frac{\left[\frac{1}{9} L_{p-free}^3 - \left(\frac{1}{3} D^3 \ln \frac{L_{p-free}}{D} + \frac{1}{9} D^3 \right) \right] u}{\frac{1}{9} L_{p-free}^3 \sqrt{gD}} \right]^{1/2}$$

1. Introduction

Aging gas pipeline installation for energy transportation is one of the main concerns in structural integrity. Any corrosion of the pipeline surface and external impact may cause an unintended release of high-pressure transported material and a sudden catch with an ignition source could result in jet fire. The jet flame characteristics including flame geometrical features, temperature profile, and radiant heat flux have been investigated for decades. In earlier research, the vertical displacement (projected flame height) of a horizontal jet flame was not always taken into account. The projected flame height was measured vertically from the nozzle to the farthest point that could be seen as shown in Figure 2.

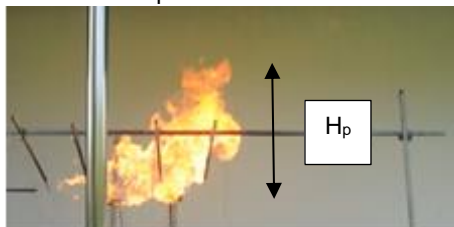


Figure 1 Projected flame height of horizontal jet flames

It was reported that with a known projected flame height data of free jet fire release, one could utilise it to estimate the likelihood of impingement area for any nearby plant installations (Ramirez-Camacho, Pastor, Casal, Amaya-Gomez, & Munoz-Giraldo, 2015). The initial work of Smith, Periasamy, Baird, and Gollahalli (2006) computed the flame dimension, including the flame height, using the image that was recorded to determine the vertical displacement. The profile values of velocity and mixture characteristics decrease with the jet distance

as the jet exits the nozzle. As a result of these reductions, buoyancy forces as well as other elements such as regional temperature and concentration differences began to predominate (Winters, 2009). The equations that are based on experimental observation for flame height estimation are then further explored by other authors that indicate parameters such as the exit diameter, ambient and fuel density, flame exit velocity and heat release rate are among the parameters quantified (Changchun et al., 2019; Ekoto, Ruggles, Creitz, & Li, 2014; Fang, Zhang, & Hu, 2023; Kim, Yang, Kim, & Won, 2009; Liu, Delichatsios, & Hu, 2019; Vijayan, Sajeevan, Thampi, & Palacios, 2024; Zhou et al., 2020). It is also revealed that the same parameters hold an important role in the flame-impinging scenario with the addition of nozzle-object separation distance (Wang et al., 2023). In addition, the flame morphology was analyzed in terms of receiving heat load and thermal stress over the impacted object. This part is however out of the scope of this paper. This study focuses on the projected flame height as influenced by variations in the release rate and separation distance of nozzle-impinged objects. A series of experiments with fuel jet velocities ranging from 17 to 42 m/s were carried out using propane as fuel released from a circular nozzle with diameter of 9.8 mm and 7.15 mm in quiescent atmospheric conditions to analyse the flame height.

2. Methodology

2.1 Experimental facility

A pressurized gas supply consisting of propane was connected through a flexible high-pressure hose to a 10-inch diameter pipe, where the gas is temporarily stored upon release and lit. The gas released was controlled using a mass-flow controller (Alicat MCR-500) installed together with a solenoid valve and a check valve to prevent gas backflow. The nozzle used was circular with a diameter of 9.8 mm and 7.15 mm. All instrumentation and measurement apparatus were checked and connected to the data acquisition system (NI 9213 with 16-Channel ± 78 mV, 24 Bit and 75 S/s aggregate was plugged into cDAQ-9178 chassis) upon the gas release. The data were acquired through LabVIEW Signal Express at 1s of sampling interval. A total of 24 tests were conducted at six different release conditions. Each test was repeated at least four times to ensure data uniformity. An anemometer was utilized to record the atmospheric conditions data. A schematic diagram of the experimental apparatus can be found in Ab Aziz and Md. Kasmani (2022).

2.2 Image processing and data fitting

Geometrical flame features that were observed in this study were the projected height (H_p). The video was recorded using the Nikon D90 SLR camera featuring a CMOS image sensor with 1,280 x 720 resolutions. The lens used, the AF-S DX NIKKOR 18-105mm f/3.5-5.6G ED VR, was pre-processed using MATLAB Image Processing Toolbox. The method of image analysis was simplified as follows; (1) Videos were rendered to 100fps (2) a hundred images for each test run were selected to be analyzed (3) Each image was processed using MATLAB Image Processing Toolbox in which raw RGB image was converted to grayscale image and adjusted to reduce the intra-class variance of grayscale image (4) Local thresholding method was used to convert the grayscale image to a binary image (5) The flame edge was determined using Sobel edge detection method (7) the flame image were combined and intermittency method was used where flame height were defined at the probability of 0.5 based on appearance probability contour (Laboureur, Gopalaswami, Zhang, Liu, & Mannan, 2016; Liu et al., 2019). Meanwhile, the regression fitting was used to observe the relationship between the y and x-axis factors.

3. Results and Discussion

Figure 2 shows the measured flame height at various strain rates (u_e/d). The evolution of flame height can be observed in two categories, free jet fire release (see Figure 2a) where no obstacle was present downstream of the jet release, and impinging jet release (see Figure 2b) where the impinging area was the head of the cylindrical vessel. It can be seen that the flame height increased as the release rate increased for free jet fire release (JFF) until it reached a point of strain rate where it was observed the flame height was decreased. The results for JFF are in good consistent with the previous findings by Changchun et al. (2019); Liu et al. (2019); Zhou et al. (2020) as presented in Figure 2a. In contrast to the previous scenario, impingement conditions resulted in a continuous increase in flame height with rising release velocity. The flame turned radially upwards and downward when it touched the surface. The releasing momentum sets the length of the radial displacement. As a result, the flame height increases as the release momentum increases, which is consistent with prior research on jet impingement by Xiaochun Zhang et al. (2017). It can be observed too that the projected flame height for the impingement scenario is higher than the free jet flame (see data for JFF and JFI_9.8a). The explanation is as follows: The free jet fire scenario (JFF) experiences higher air entrainment compared to impinging jet (JFI_9.8a), which is consistent with findings from a prior study of impinging jet on the inclined

tunnel (Kong, Wang, Cong, Liu, & Zhu, 2019). Other studies of air entrainment with sidewalls near the jet flame have also validated that air entrainment is inversely proportional to flame geometry (Tao, Shen, & Zong, 2016). For the jet fire impingement scenario, the presence of an object downstream reduces air entrainment, resulting in a higher flame height.

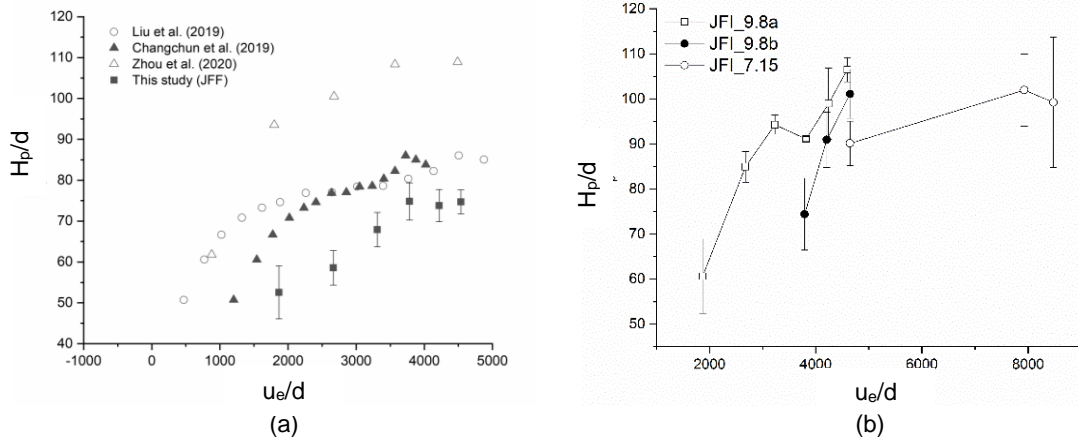


Figure 2 Dimensionless flame height against strain rate for (a) free jet fire release (JFF) plotted with previous findings of Liu et al. (2019), Changchun et al. (2019); Zhou et al. (2020) and (b) impinging jet release (JFI)

The binary images that are shown in Figure 3 (a), (b), and (c) were created from the pre-processed images using the MATLAB Image Processing Toolbox. It is evident that, despite the similarity in release flow rate across all scenarios, variations in release diameter and nozzle to target distance have a notable impact on the resulting flame pattern and dimensions.

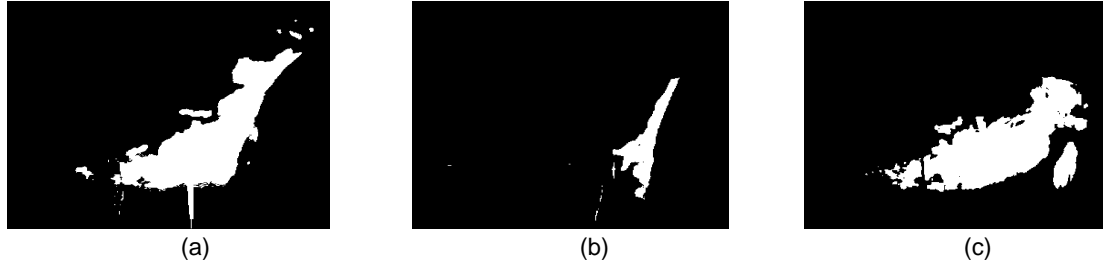


Figure 3 Pre-processed image of (a) JFI_9.8a and (b) JFI_7.15 (c) JFI_9.8b at similar release flowrate

The measurement of the flame extension length as it reaches the impingement point was determined by quantifying the amount of unburned fuel remaining after impingement, as well as the quantity of unburned fuel while moving along the impinging surface. Thus, for an impinging jet, a relationship between the height of the flame and the amount of fuel left unburned after the impingement point is represented in Eq (1) (Xiaochun Zhang et al., 2017);

$$\frac{H_p}{D} \sim fcn \left(\frac{V_{fu}}{V_f} \dot{Q} \right) \quad (1)$$

where H_p is the projected flame height, D is the nozzle-to-object separation distance, V_{fu} is the flame volume portion intercepted by the impinging surface in m^3 , and V_f is the volume of the free flame in m^3 . For a horizontal and inclined surface, the region where the flame is intercepted, an ideal geometry such as cylinder and ellipse was used to represent the flame volume (Qiu, Hu, Chen, & Carvel, 2018; Xiaolei Zhang, Hu, Delichatsios, & Zhang, 2019; Xiaochun Zhang, Hu, Zhu, Zhang, & Yang, 2014; Xiaochun Zhang et al., 2017). The following Eq (2) and (3) correlate the upward flame height after impingement points for cylindrical and elliptical flame shapes, respectively.

$$\frac{H_p}{d} \sim \frac{1}{2} \left[\frac{(L_{p-free} - D)u_e}{L_{p-free}\sqrt{gD}} \right]^{1/2} \quad (2)$$

$$\frac{H_p}{d} \sim \left[\frac{\left[\frac{1}{9} L_{p-free}^3 - \left(\frac{1}{3} D^3 \ln \frac{L_{p-free}}{D} + \frac{1}{9} D^3 \right) \right] u_e}{\frac{1}{9} L_{p-free}^3 \sqrt{gD}} \right]^{1/2} \quad (3)$$

From the study of Xiaochun Zhang, Hu, Zhu, et al. (2014), the cylindrical flame shape was an ideal assumption for a vertical jet impingement on a horizontal ceiling with a wider range of $([(L_t - D)/d])$ from 0 to 14.5 as compared to the study done by You and Faeth (1979) which ranges between 0 to 5.8. In this study, a higher range of $([(L_t - D)/d])$ was used to test and extend the previous correlation applicability for larger-scale jet impingement release. The range used is between 20 to 110. Higher $([(L_t - D)/d])$ indicates a larger scale of impingement release. Based on Figure 4, a comparison was done to fit data in this study with the Eq (2) and Eq (3). From both figures, the elliptical flame shape assumption gives a better fit with an R^2 value of 0.97. However, the data of the release nozzle of 7.15 mm (JFI_7.15) fit the previous correlation of Xiaochun Zhang, Hu, Zhang, Yang, and Wang (2014). This is due to the smaller nozzle producing a thinner flame volume visibility, and this will influence the flame height (refer to Figure 3).

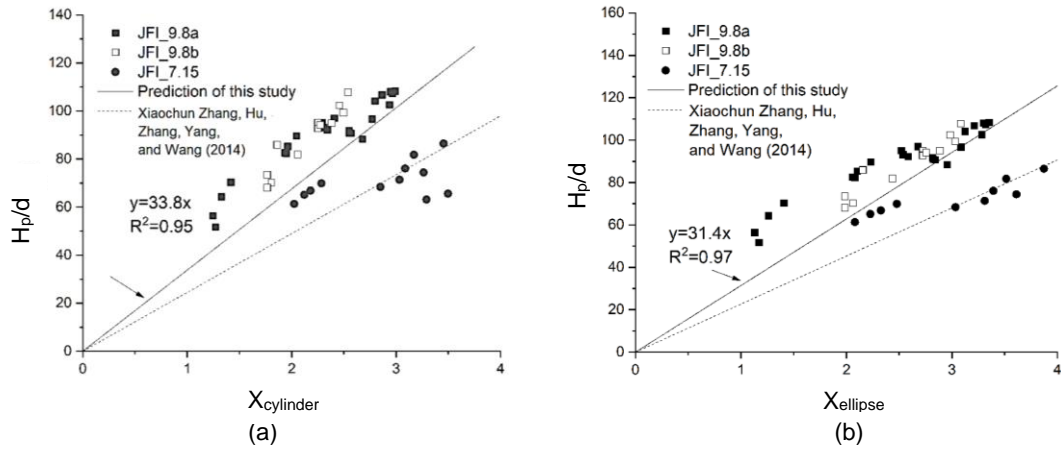


Figure 4 Dimensionless association between the upward flame height and the ideal flame shape assumption (a) cylindrical and (b) elliptical on an impinged surface.

From Figure 4, a new constant of 31.4 was introduced to give a better fit on the influence of impingement to the flame height using an elliptical flame shape as follows;

$$\frac{H_p}{d} \sim 31.4 \left[\frac{\left[\frac{1}{9} L_{p-free}^3 - \left(\frac{1}{3} D^3 \ln \frac{L_{p-free}}{D} + \frac{1}{9} D^3 \right) \right] u}{\frac{1}{9} L_{p-free}^3 \sqrt{gD}} \right]^{1/2} \quad (4)$$

It can be said that the flame impingement gave an elliptical flame shape instead of cylindrical and thus, Eq (4) could be used to estimate the projected flame height of the impinging jet flame. Further data fitting was done by using theoretical assumption as has been done by other previous studies of Kim et al. (2009); Liu et al. (2019) by using the following model

$$\tan \theta = \frac{1}{\sqrt{\frac{\rho_0}{\rho_\infty} Fr^*}} \left[\left(\frac{s}{d} \right) + 2\beta \left(\frac{s}{d} \right)^2 + \frac{4}{3} \beta^2 \left(\frac{s}{d} \right)^3 \right] \quad (5)$$

Where the tilt angle, θ at designated coordinates, s were dependent on the exit diameter, d , and modified Froude number, Fr^* . Thus, the data in this study were also fitted in the Eq (5) and the observation for free jet fire release can be seen in Figure 5a while for impingement scenario can be seen in Figure 5b.

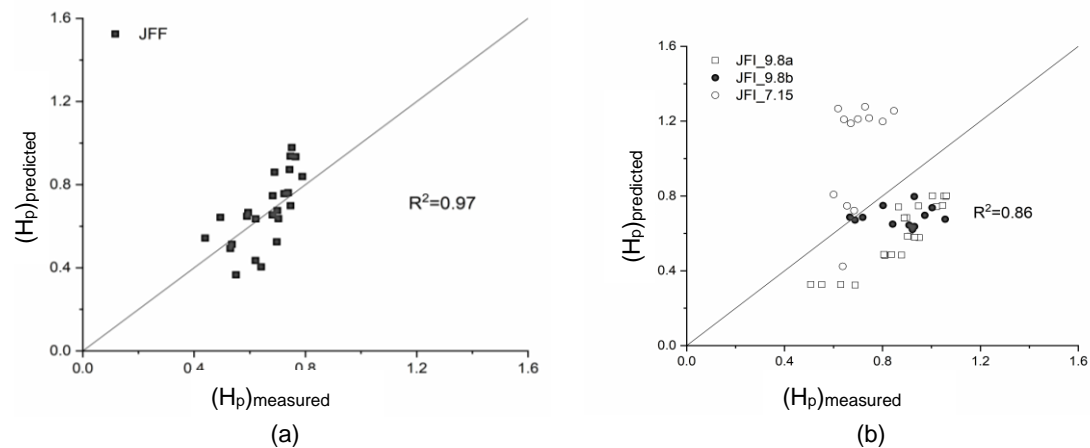


Figure 5 Graph of predicted against measured value of H_p for (a) free jet fire release (b) impinging jet release.

In the case of a free jet fire release, it is evident that the flame integral model's theoretical assumption is suitable for predicting H_p , as evidenced by an R^2 value of 0.97. Conversely, in the scenario of impingement, the R^2 value is 0.86. In the impinging scenario, the H_p data were compared to the predictions obtained from Eq (4), resulting in a higher level of agreement with an R^2 value of 0.98 as shown in Figure 6. The aforementioned observation provides additional support for the utilization of Eq (4) for the prediction of the flame extension length. In the present study, the term "flame height" is employed instead of the conventional term "flame extension length" due to variations in orientation compared to previous investigations.

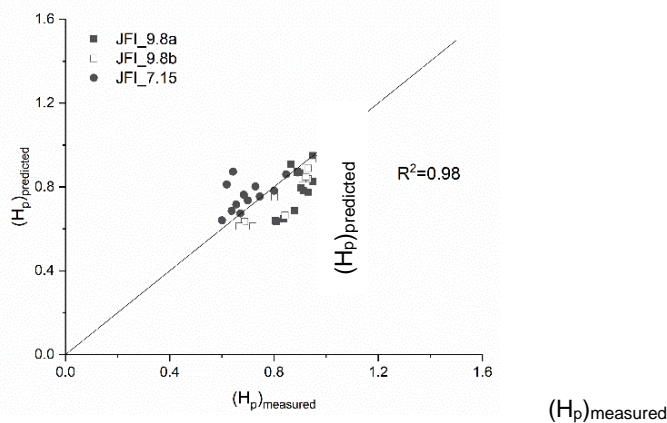


Figure 6 Comparison of predicted and measured values of H_p by employing elliptical flame shape assumption for impinging jet fire.

4. Conclusion

This paper presents the experimental results that elucidate the fuel velocity and nozzle exit size on the anticipated flame height H_p , it was found that the projection was inconsistent or discordant with the actual value. Experimental data indicated an initial increase in H_p value followed by a subsequent decline. When the separation gap was smaller, the H_p for an impinging scenario was larger. The quantity of unburned fuel would influence the H_p since the initial momentum of the discharged fuel is conserved. It is evident that with a greater release rate, there is more unburned fuel at the moment of impingement, which results in higher H_p . The H_p equation should be utilised with caution because this condition could not be seen using H_p prediction. The laminar oscillation field, followed by the turbulent and momentum-dominated zones, interleaves the flow regimes as the nozzle exit velocity rises. As proposed, the Eq (4) can be used to correlate the predicted flame height for an impingement situation utilizing an elliptical flame shape.

Acknowledgments

The authors gratefully acknowledge the financial support provided by the College of Engineering, UiTM.

References

- Ab Aziz, N. S., & Md. Kasmani, R. (2022). The effects of geometrical flame feature on radiant heat flux prediction of horizontal jet flames using line source model. *Process Safety Progress*, *41*, S45-S52.
- Changchun, L., Tiandiao, D., Shasha, Z., Xinlei, L., Jun, D., Zhenmin, L., & Li, M. (2019). Radiation Model of Horizontal Jet Flame Governed by Buoyancy and Momentum. *Journal of Heat Transfer*, *141*(11). doi:10.1115/1.4044512
- Ekoto, I. W., Ruggles, A. J., Creitz, L. W., & Li, J. X. (2014). Updated jet flame radiation modeling with buoyancy corrections. *International Journal of Hydrogen Energy*, *39*(35), 20570-20577. doi:10.1016/j.ijhydene.2014.03.235
- Fang, X., Zhang, X., & Hu, L. (2023). Transitional behavior of vertical flame height of horizontally-oriented rectangular-source jet fires. *Proceedings of the Combustion Institute*, *39*(3), 3969-3980.
- Kim, J., Yang, W., Kim, Y., & Won, S. (2009). Behavior of buoyancy and momentum controlled hydrogen jets and flames emitted into the quiescent atmosphere. *Journal of Loss Prevention in the Process Industries*, *22*(6), 943-949.
- Kong, X. X., Wang, X. S., Cong, H. Y., Liu, Y. P., & Zhu, J. P. (2019). Temperature profile and flame extension length of a ceiling impinging round jet fire in an inclined tunnel. *International Journal of Thermal Sciences*, *137*, 526-533. doi:10.1016/j.ijthermalsci.2018.12.023
- Laboureur, D. M., Gopalaswami, N., Zhang, B., Liu, Y., & Mannan, M. S. (2016). Experimental study on propane jet fire hazards: Assessment of the main geometrical features of horizontal jet flames. *Journal of Loss Prevention in the Process Industries*, *41*, 355-364. doi:10.1016/j.jlp.2016.02.013
- Liu, S., Delichatsios, M. A., & Hu, L. (2019). Flame profile parameters of horizontal turbulent jets: Experiments, similarity analysis and an integral model. *Combustion and Flame*, *207*, 1-9. doi:10.1016/j.combustflame.2019.05.029
- Qiu, A., Hu, L., Chen, L., & Carvel, R. O. (2018). Flame extension lengths beneath a confined ceiling induced by fire in a channel with longitudinal air flow. *Fire Safety Journal*, *97*, 29-43.
- Ramirez-Camacho, J. G., Pastor, E., Casal, J., Amaya-Gomez, R., & Munoz-Giraldo, F. (2015). Analysis of domino effect in pipelines. *Journal of Hazardous Materials*, *298*, 210-220. doi:10.1016/j.jhazmat.2015.05.033
- Smith, T., Periasamy, C., Baird, B., & Gollahalli, S. R. (2006). Trajectory and Characteristics of Buoyancy and Momentum Dominated Horizontal Jet Flames From Circular and Elliptic Burners. *Journal of Energy Resources Technology*, *128*, 300-310. doi:10.1115/1.2358145
- Tao, C. F., Shen, Y., & Zong, R. W. (2016). Experimental study on virtual origins of buoyancy-controlled jet flames with sidewalls. *Applied Thermal Engineering*, *106*, 1088-1093. doi:10.1016/j.applthermaleng.2016.06.072
- Vijayan, P., Sajeevan, A. C., Thampi, G., & Palacios, A. (2024). Experimental evaluation of subsonic-horizontal jet flames: Impact of practical crack shapes. *Fire Safety Journal*, 104127.
- Wang, Z., Jiang, J., Wang, G., Ni, L., Pan, Y., & Li, M. (2023). Flame morphologic characteristics of horizontally oriented jet fires impinging on a vertical plate: Experiments and theoretical analysis. *Energy*, *264*, 126210.
- Winters, W. S. (2009). *Modeling leaks from liquid hydrogen storage systems*. Retrieved from
- You, H., & Faeth, G. (1979). Ceiling heat transfer during fire plume and fire impingement. *Fire and Materials*, *3*(3), 140-147.
- Zhang, X., Hu, L., Delichatsios, M. A., & Zhang, J. (2019). Experimental study and analysis on flame lengths induced by wall-attached fire impinging upon an inclined ceiling. *Proceedings of the Combustion Institute*, *37*(3), 3879-3887. doi:10.1016/j.proci.2018.06.203
- Zhang, X., Hu, L., Zhang, X., Yang, L., & Wang, S. (2014). Non-dimensional correlations on flame height and axial temperature profile of a buoyant turbulent line-source jet fire plume. *Journal of Fire Sciences*, *32*(5), 406-416.
- Zhang, X., Hu, L., Zhu, W., Zhang, X., & Yang, L. (2014). Flame extension length and temperature profile in thermal impinging flow of buoyant round jet upon a horizontal plate. *Applied Thermal Engineering*, *73*(1), 15-22. doi:10.1016/j.applthermaleng.2014.07.016
- Zhang, X., Tao, H., Xu, W., Liu, X., Li, X., Zhang, X., & Hu, L. (2017). Flame extension lengths beneath an inclined ceiling induced by rectangular-source fires. *Combustion and Flame*, *176*, 349-357.
- Zhou, K., Wang, Y., Zhang, L., Wu, Y., Nie, X., & Jiang, J. (2020). Effect of nozzle exit shape on the geometrical features of horizontal turbulent jet flame. *Fuel*, *260*. doi:10.1016/j.fuel.2019.116356